Article:
Califano, M orcid.org/0000-0003-3199-3896, Lu, R and Zhou, Y (2021) Indirect to Direct Band Gap Transformation by Surface Engineering in Semiconductor Nanostructures. ACS Nano, 15 (12). pp. 20181-20191. ISSN 1936-0851

https://doi.org/10.1021/acsnano.1c08176

Supporting Information for: Indirect to Direct Band Gap Transformation by Surface Engineering in Semiconductor Nanostructures

Marco Califano,[*,†,‡] Ruiyan Lu,[¶] and Yeke Zhou[¶]

† *Pollard Institute, School of Electronic and Electrical Engineering, University of Leeds, Leeds LS2 9JT, United Kingdom*

‡ *Bragg Centre for Materials Research University of Leeds, Leeds LS2 9JT, United Kingdom*

¶ *School of Electronic and Electrical Engineering, University of Leeds, Leeds LS2 9JT, United Kingdom*

E-mail: m.califano@leeds.ac.uk

Origin of the features in the optical spectra calculated for GaP NCs with different surface stoichiometries

In both Ga-rich and P-rich NCs, each peak in the emission and the absorption spectrum can be decomposed into several smaller peaks (denoted in the figure by numbers, increasing with the peak's position in energy), each of which, in turn, is contributed to by many different transitions (identified, for the case of the emission, by numbered arrows in the insets of Fig.4 - main text).

Focussing on the PL (*i.e.*, the blue curves) first, we see that the emission in NCs with Ga-rich surfaces (Fig.4a, main text) originates from transitions to the X-like CBM from a large set of prevalently Γ-like VB states, starting from the degenerate VBM ($|h_{1,2}\rangle$), including nearly all states down to $|h_{13}\rangle$, and spanning an energy of 190 meV. In contrast, in NCs with P-rich surfaces (Fig.4b, main text), emission involves transitions to two CB states - the singly-degenerate Γ-like CBM and the 3-fold degenerate (without accounting for spin) X-like CBM+1 - from a smaller set of VB states ($|h_{1,2}\rangle - |h_6\rangle$) with strong Γ character. As we already mentioned, the absorption edge in this type of NCs originates from the same transitions as the PL, whereas the next broad shoulder (again decomposed into smaller peaks - numbered 4 to 7 - in Fig.4b, main text), receives sizeable contributions from a much wider range of transitions, involving conduction states from $|e_1\rangle$ (*i.e.*, the CBM), up to $|e_{13}\rangle$, and valence states from the VBM ($|h_{1,2}\rangle$) down to $|h_{15,16}\rangle$. In NCs with Ga-rich surfaces, instead, the main shoulder in absorption (located at 350-360 nm in Fig.4a - main text - and decomposed into the peaks labelled 1 to 4) is contributed to by a very large number of transitions (including CB states as high as $|e_{23}\rangle$, and VB states as deep as $|h_{20}\rangle$), the strongest of which, however, involve all the Γ-like CB state (which for this specific dot size is state $|e_{20}\rangle$). The long tail (that extends to about 430 nm in Fig.4a, main text, and whose 'fine structure' - dashed red line - has been magnified 50 fold in the figure) only involves transitions to X-like states.

From this description it is therefore clear that the picture of the transitions responsible for the features observed in the optical spectra of GaP NCs that emerges from an accurate atomistic modelling, where each electron state is represented as a superposition of 3D bulk X-like, L-like and Γ-like Bloch states (see Fig.3, main text), is much more complex than that obtained from simplified approaches,[1,2] where the states are assumed to be modified single-valley bulk states. Indeed, Kim *et al.*,[1] based on the effective mass approximation, attributed the features they observed in the absorption spectra of GaP NCs (*i.e.*, the main shoulder and the long tail), to only 4 transitions: the direct Γ_{8v} to Γ_{1c} and Γ_{7v} to Γ_{1c} described the shoulder, and the indirect Γ_{8v} to X_{1c} and Γ_{7v} to X_{1c} were responsible for the tail. They therefore identified the peaks splitting as due to the extra transitions originating from the spin-orbit split-off valence band Γ_{7v}. If that were the case, however, both peaks splitting should be exactly the same and equal to $E(\Gamma_{8v}) - E(\Gamma_{7v})$ (= 80 meV in bulk GaP[3]). Instead, the measured splittings are different (125 and 182 meV), and in disagreement with the measured SO splitting in bulk GaP.

Passivation procedure and parameters

The unsaturated bonds at the dot surface are passivated here using pseudo-hydrogenic, short-range potentials with Gaussian form,

$$v(\mathbf{r}) = \alpha e^{-(|\mathbf{r}-\mathbf{R}(\gamma)|/\sigma)^2} \tag{S1}$$

As any surface atom with only one bond (*i.e.*, with three dangling bonds, in the case of materials with the zinc blende crystal structure) is removed from the structure because of its instability towards dissociation, we have only 4 types of passivants: c1, c2, a1, and a2, for cations (c) and anions (a) with one and two dangling bonds, respectively. Each passivant is characterized by (i) the amplitude α (in hartree) and (ii) the width σ (in Bohr) of the Gaussian potential, and by (iii) the distance γd from the surface atom along the

ideal bond line connecting it with the missing atom (d is the bond length and $\mathbf{R}(\gamma)$ is the ligand position).[4] As the electronic structure calculations are performed in reciprocal space, Eq. (S1) needs to be Fourier transformed into[4]

$$v(\mathbf{q}) = \alpha\pi^{1.5}\sigma^3 e^{i\mathbf{q}\cdot\mathbf{R}} e^{-(\sigma|\mathbf{q}|/2)^2} \tag{S2}$$

to obtain the relationship between real-space parameters and q-space ones (which are the actual input to the calculations): $a = \alpha\pi^{1.5}\sigma^3$, $b = \sigma/2$, and $c = \gamma$. For a more detailed explanation of the passivation procedure and the values of the different parameters, we refer the reader to 4. In brief: the distances c_i, being fractions of the ideal bond distance, vary from 0.1 to 1; the range of b_i is $[0.1, 1.5]$ and is determined by the condition that the potential must decay to zero as both $|q|$ and $|r|$ become large; finally, the amplitudes a_i are positive for the cations (which have lower electronegativity than the anions) to ensure that they lose electrons, whereas negative for the anions, to ensure that they gain extra electrons. Their variation range depends on the bulk pseudopotential of the specific atom they passivate.[4]

Once these parameters are determined for each passivant, through an optimisation process carried out on an ensemble of representative test structures, they are used for any NC size of the same material.

Table S 1: Passivation parameters used to passivate surface Ga, P, Al and As atoms in this work. For both GaP and AlAs we use two passivation sets: ideal passivants (ip), and electronegative passivants (ep). For GaP the ep set is obtained by choosing a slightly more negative passivation potential for the surface anion with two dangling bonds (its value is changed from -0.8 in the ip to -1.0, highlighted in red in the table), whereas for AlAs, where that potential has already a large negative value in the ip set, the ep set is obtained by simply moving the passivant closer to the surface anion with two dangling bonds (from 0.6 to 0.15 of the ideal bond distance, change highlighted in red in the table).

Passivation	cation						anion					
	1 dangling bond†			2 dangling bonds†			1 dangling bond†			2 dangling bonds†		
	a	b	c	a	b	c	a	b	c	a	b	c
GaP (ip)	0.50	0.50	0.70	0.50	0.15	0.25	-0.60	0.55	0.30	-0.80	0.30	0.20
GaP (ep)	0.50	0.50	0.70	0.50	0.15	0.25	-0.60	0.55	0.30	-1.00	0.30	0.20
AlAs (ip)	1.90	0.50	0.10	2.00	0.30	0.20	-2.00	0.60	0.40	-2.00	0.50	0.60
AlAs (ep)	1.90	0.50	0.10	2.00	0.30	0.20	-2.00	0.60	0.40	-2.00	0.50	0.15

† Surface atoms with 3 dangling bonds were removed as they are unstable for dissociation.

Surface composition of our GaP NCs

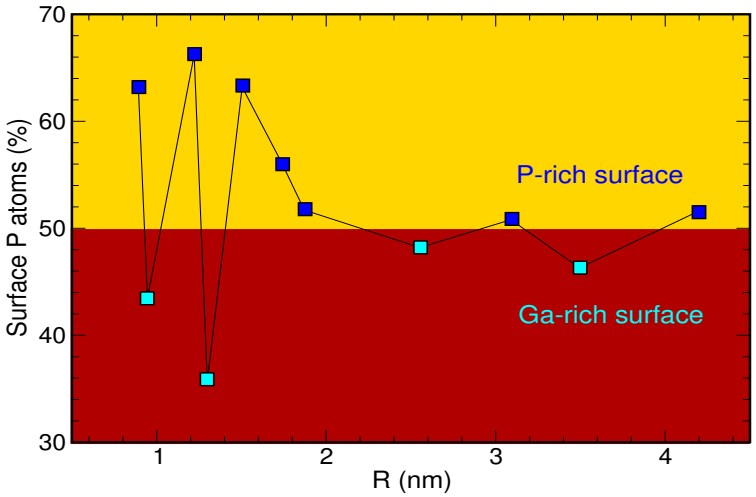

Figure S 1: Surface composition of representative GaP NCs with radii ranging from 0.9 to 4.2 nm, expressed in terms of the ratio ($\times$100) between the number of surface P atoms and the total number of surface atoms. Owing to the spherical-like shape of the nanostructures and the material's crystal structure, each NC surface has an excess of either cations or anions, depending on the size of the radius: NCs with P-rich surfaces (blue squares) lay in the top part of the plot (yellow background), whereas NCs with Ga-rich surfaces (cyan squares) lay in the bottom part of the graph (burgundy background). In zincblende materials these anion- or cation-rich facets are oriented along the (100), (010), (001) and equivalent directions, as shown in Fig.1 (main text).

Difference between surface (gap) states and core states

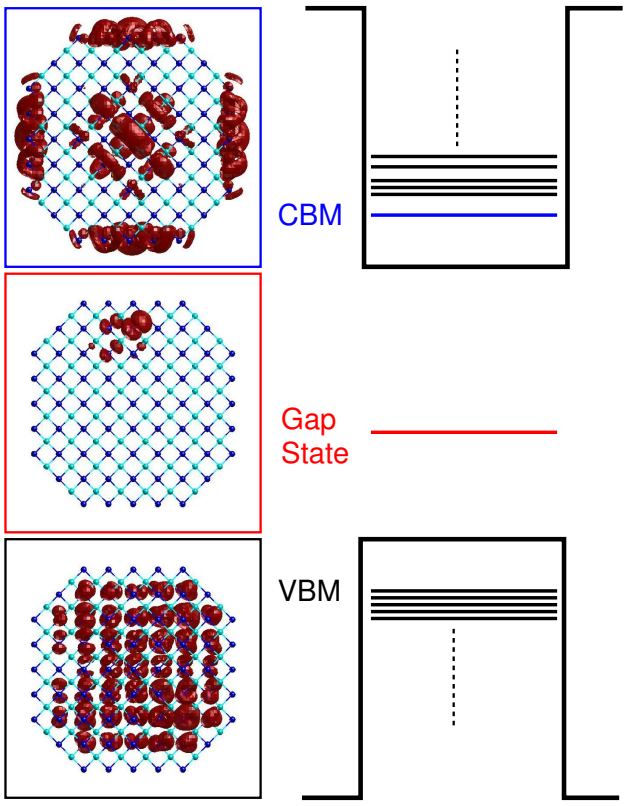

Figure S 2: Charge density distribution calculated for the band edges (CBM and VBM) and a gap state (generated by removing a surface passivant) in a GaP NC with $R = 1.2$ nm and a P-rich surface. It is clear that, apart from their energetic positions, which identify their nature, the character of these states can also be deduced from their different spatial distribution: Indeed whilst core states are delocalised over a large volume (even in the case of the more shell-like localisation of the CBM, specific for this particular case), a gap state exhibits a strong localisation around a few surface atoms. This shows that: (i) the CBM we obtain in GaP NCs with P-rich surfaces is not a gap state; and (ii) the passivation parameters adopted for GaP NCs are effective at removing states from the gap, which is their main purpose.

References

(1) Kim, S.; Lee, K.; Kim, S.; Kwon, O.-Pil; Heo, J.H.; Im, S.H.; Jeong, S.; Lee, Doh C.; Kim, S.-W. Origin of Photoluminescence from Colloidal Gallium Phosphide Nanocrystals Synthesized *via* a Hot-Injection Method *RSC Adv.*, **2015**, *5*, 2466-2469.

(2) Krishna, M.V.R.; Friesner, R.A. Quantum Confinement Effects in Semiconductor Clusters. *J. Chem. Phys.* **1991**, *95*, 8309-8322.

(3) Intrinsic Properties of Group IV Elements and III-V, II-VI and I-VII Compounds. In *Landolt- Börnstein - Numerical Data and Functional Relationships in Science and Technology - Group III: Crystal and Solid State Physics*, Madelung, O.; von der Osten, W.; Rössler, U., Eds.; Springer-Verlag: Berlin Heidelberg (Germany), 1987; Vol. 22A.

(4) Graf, P.A.; Kim, K.; Jones, W.B.; Wang, L.W. Surface Passivation Optimization Using DIRECT. *J. Comput. Phys.* **2007**, *224*, 824-835.